Colorimetric Cu²⁺ Detection of (1*E*,2*E*)-1,2-Bis((1*H*-pyrrol-2-yl)methylene)hydrazine Using a Custom-Built Colorimeter

Sasipan Luangphai, Jaturon Fongsiang, Pumis Thuptimdang, Sasiwimon Buddhiranon, and Kullapa Chanawanno*

ABSTRACT: The compound (1*E*,2*E*)-1,2-bis((1*H*-pyrrol-2-yl)-methylene)hydrazine (**1**) was investigated for its chemosensor application. The colorimetric response of **1** with various ions was investigated, and the selective optical change upon mixing with Cu²⁺ was found. The Cu²⁺ binding stoichiometry of **1** derived from Job's plot and the *in silico* study give us the tentative structural detail of the binding mode of **1** and Cu²⁺ being 1:1. The binding constant between **1** and Cu²⁺ from the Benesi−Hildebrand plot was 1.49×10^4 M^{-1}. The limit of detection of **1** in Cu²⁺ detection was 0.64 μM (0.040 ppm), which is much lower than the WHO and US EPA maximum allowable Cu²⁺ level in drinking water (2 and 1.3 ppm, respectively). The custom-built colorimeter demonstrates a good linear relationship between Cu²⁺ concentration and electrical resistance (Ω) upon **1**−Cu²⁺ ion binding.
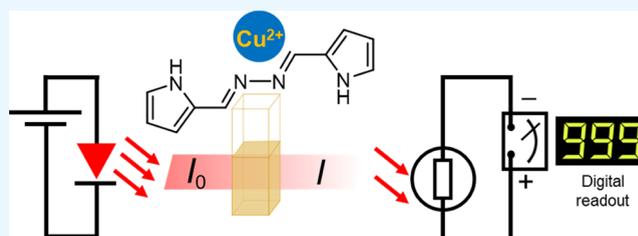
1. INTRODUCTION

Colorimetric chemosensors are a fast-growing topic of study. There has been a great quantity of compound library that has a potential use for many various forms of analysis. One of the factors driving advancement in the sector is the high cost of analytical methods used to quantify the analytes. The cost comparison between the real-time polymerase chain reaction (RT-PCR) method and antigen test kit for some medical examination is a good example.[1−4] In a developing nation, the costly, time-consuming, and inconvenient technique would prevent many patients from receiving an accurate diagnosis, resulting in a greater death rate than in first-world countries. Fast, yet reliable detection procedures at a cheap cost can assist users with no background in the operation by allowing them to conduct the detection with limited resources.

The selective detection of Cu²⁺ ions has attracted the attention of scientists. The copper (II) ion is an important trace element for humans in low quantities. However, at an excessive level, it becomes a poisonous and dangerous substance to organisms and the environment. Furthermore, Cu²⁺ may accumulate in human and animal livers via bioaccumulation or biomagnification, causing cell death and a variety of neurological illnesses such as Alzheimer's disease, as well as heart disease, liver and kidney damages, Menkes syndrome, Wilson's disease, Huntington disease, and others.[5−11] According to the World Health Organization (WHO), the maximum acceptable quantity of Cu²⁺ in drinking water is 2.0 ppm.[12]

Hydrazone- and azomethine-related functional groups are widely used in sensor research due to their high modularity and ease of production.[13] Because of their numerous binding sites and variable conformation, the dimeric hydrazine Schiff base structural motifs (Figure 1a) are excellent for cation sensing. The nucleophilic nitrogen in both imine and amine in **1** are capable of forming an adduct with Lewis acid such as cations and metal ions. The presence of pyrrole rings as a strong nucleophile should also promote metal ion binding. In 2014, Ziegler et al.[14] reported the unique BF₂-based fluorophore called bis(difluoroboron)-1,2-bis((1*H*-pyrrol-2-yl)methylene)hydrazine or BOPHY (Figure 1b). In the BOPHY model, boron binding mode adopted a six-membered-ring chelate formation integrating the BF₂ group, *N*-pyrrole, and *N*-imine from the hydrazone ligand. The flexibility of ligand **1** promotes the BF₂ adduct formation and results in a very optically stable BOPHY. Since the BOPHY dye discovery in 2014, it has been functionalized and sporadically used as a chemical sensor.[15−18] To the best of our knowledge, ligand **1** has never been used in a detailed chemosensor study so we decided to use it in our work. For ligand **1**, the pyrrole units should bind to the analytes, expectedly a Lewis acid, forming a rigid dipyrrin-like skeleton similar to the well-known boron dipyrromethene BODIPY and
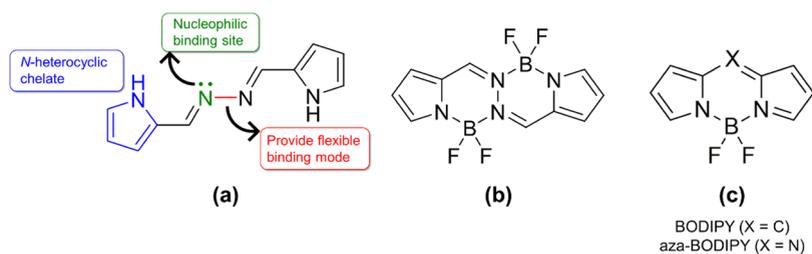
Figure 1. (a) Structure of **1** and its potential factors for ion sensing ability, (b) BOPHY, and (c) BODIPY and aza-BODIPY cores.

aza-BODIPY dyes (Figure 1c). The photophysical properties of BODIPY derivatives are excellent for this skeleton.

2. EXPERIMENTAL SECTION

2.1. Materials and Instrumentation. Solvents and starting materials (AR grade) for syntheses were purchased commercially and used as received. ^{1}H NMR spectra were recorded on a Bruker DRX-400 NMR spectrometer in CDCl$_3$ solution with tetramethylsilane ($\delta = 0.00$ ppm) as an internal standard. The UV–vis spectra were recorded on Thermo Scientific Evolution TM 201/220 in the range of 300–800 nm. FTIR spectra were using a Bruker Tensor 27 FTIR spectrometer in the range of 4000–500 cm^{-1}.

2.2. Synthesis of 1 ((1E,2E)-1,2-Bis((1H-pyrrol-2-yl)-methylene)hydrazine). Pyrrole-2-carbaldehyde (1.00 g, 10.5 mmol), hydrazine hydrate (0.30 g, 6.0 mmol), and 30 mL of ethanol were mixed. Catalytic amount of acetic acid was added into the mixture (Scheme 1). The resulting mixture gradually

Scheme 1. Synthesis of Compound 1
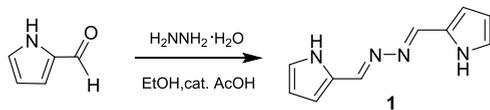
turned yellow in a few minutes and some yellow precipitate started to appear. The reaction was monitored using a TLC technique and was completed in 1 h. The solid was filtered, washed with 10 mL diethyl ether twice, and air-dried. The compound was flash-crystalized and washed again to get 0.72 g of fine yellow crystal (yield 64%).

2.3. Colorimetric Response Study. All spectroscopic studies were conducted using ethanolic solutions. The sensing ability of compound **1** was investigated using Cu^{2+}, Ba^{2+}, Co^{2+}, K$^+$, Na$^+$, Mn^{2+}, Ni^{2+}, Zn^{2+}, Cr^{2+}, Ag$^+$, Ca^{2+}, Mg^{2+}, Al^{3+}, NH$_4^+$, OH$^-$, NO$_3^-$, NO$_2^-$, SO$_4^{2-}$, Cl$^-$, PO$_4^{3-}$, and CH$_3$COO$^-$. Compound **1** and all metal salts were dissolved in ethanol, and the concentration was adjusted to 0.013 mM. The mixture of **1** and each ion was shaken, and the corresponding spectral changes were monitored using a UV–vis spectrometer.

UV–vis spectrophotometric titration upon the addition of Cu(CO$_2$CH$_3$)$_2$·H$_2$O solution was conducted directly in a 2 mL quartz cuvette by successive addition of corresponding ion solution using a microliter pipette. The solution was well mixed after each aliquot addition, and the spectrum was recorded. All experiments were carried out at room temperature.

2.4. Stoichiometric Study. The Job's plot method was employed to determine the stoichiometric ratio of the coordination between **1** and Cu^{2+} ion. The stock solution of equimolar (27 μM) of both **1** and Cu^{2+} was mixed at different

volume ratios with a total mixed volume of 1 mL. The absorbance of various **1**–**Cu** mixture at 438 nm was recorded, and the plot between the absorbance and mole ratio of **1** (χ_1) was made. Each χ_1 can be calculated from eq 1.[19]

$$\chi_1 = \frac{\text{mole } \mathbf{1}}{\text{mole } \mathbf{1} + \text{mole } Cu^{2+}} \qquad (1)$$

2.5. Detection Limit and Binding Constant Determination. The detection limit of **1** toward the Cu^{2+} sensing was calculated by monitoring the change in the absorbance titration method using various concentrations of Cu^{2+} ions at 438 nm. The detection limit can be calculated using eq 2

$$\text{detection limit} = \frac{3\text{SD}}{m} \qquad (2)$$

where SD is the standard deviation of the blank measurement and m is the slope of the plot of the absorbance versus Cu^{2+} concentration.

The binding constant (K_a) was calculated according to the Benesi–Hildebrand plot using eq 3

$$\frac{1}{A - A_0} = \frac{1}{K_a(A_{max} - A_0)[Cu^{2+}]} + \frac{1}{A_{max} - A_0} \qquad (3)$$

where A_0 is the absorption of **1** in the absence of Cu^{2+}, A is the absorbance of the mixture of **1** and Cu^{2+} at various concentrations, A_{max} is the absorbance of the mixture in the presence of highest [Cu^{2+}], and K_a is the binding constant in the unit of M^{-1}. The K_a can be calculated from the slope of a straight line plot of $1/(A - A_0)$ and $1/[Cu^{2+}]$.

2.6. Computational Study. To estimate the conformational nature of the dyes **1** and Cu^{2+} in ethanolic solution, we conducted the *in silico* study to confirm the propose bonding mode of **1**–**Cu**. The molecular geometry of **1**–**Cu** was optimized using Avogadro 1.2.0 software.[20] And the molecular mechanics energy was calculated using universal force field (UFF).

2.7. Custom-Built Colorimeter. The low-cost colorimeter was assembled using a light-dependent resistor (LDR) as a light detector. When exposed to light, the LDR sensor's electrical resistance decreases.[21] The aim of making this device is to see whether the linear relationship between the resistances in ohm (Ω) derived from the LDR and the concentration of Cu^{2+} could be obtained. The idea of the colorimeter is based on the Beer–Lambert law, in which the solution with pale color would give a high intense light (I) compared with the initial input light (I_0, see Figure 2). The higher light intensity would result in a lower current resistance due to a large amount of current that can flow through the LDR.[22−24]
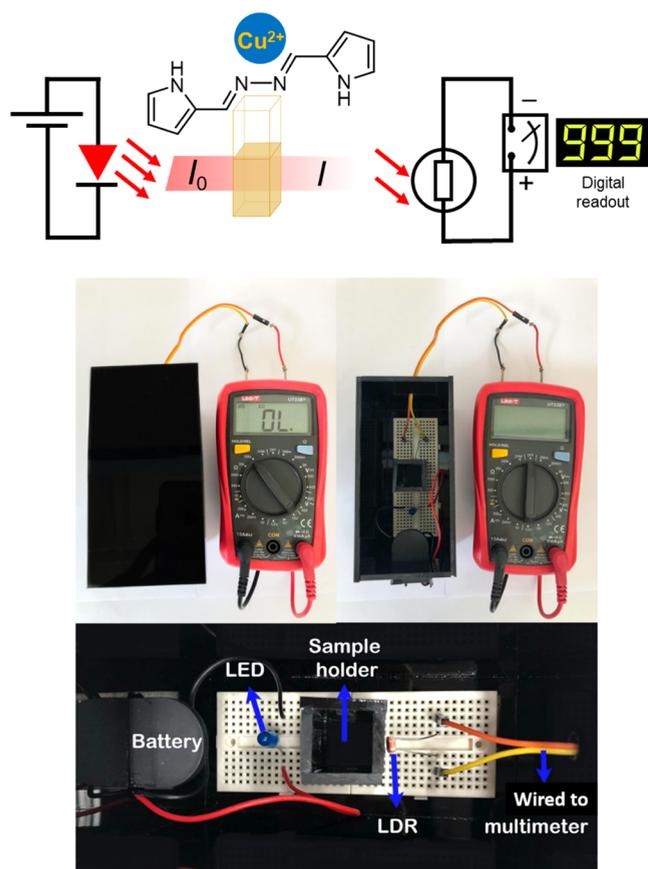
Figure 2. Schematic diagram and the homemade colorimeter.

3. RESULTS AND DISCUSSION

The simple one-pot synthesis enables us to generate a high purity product with a reasonable yield. Our ^1H NMR data (Figure S1) is consistent with the reported compound.[14] δ_H 400 MHz in $CDCl_3$ (multiplicity, assign.): 6.99 (m, 2H), 6.18−6.20 (m, 2H), 6.61 (m, 2H), 8.39 (s, 2H), 11.58 (bs, 2H).

3.1. Spectroscopic Studies of Metal Sensing. An ethanolic solution (0.54 mM) of **1** and different cations and anions (Cu^{2+}, Ba^{2+}, Co^{2+}, K^+, Na^+, Mn^{2+}, Ni^{2+}, Zn^{2+}, Cr^{2+}, Ag^+,

Ca^{2+}, Mg^{2+}, Al^{3+}, NH_4^+, OH^-, NO_3^-, NO_2^-, SO_4^{2-}, Cl^-, PO_4^{3-}, CH_3COO^-) were mixed in glass vials. We found that when we added Cu^{2+} solution, the color of **1** rapidly changed to a vivid orange that could be seen with the naked eye, but the other mixture exhibited no color change (Figures 3 and S3). The results showed that compound **1** could be used as a naked eye colorimetric sensor with high Cu^{2+} selectivity. With the progressive increase in absorbance at 438 nm, the spectral data verifies the naked eye observation (Figure 4). At roughly 405 nm, the isosbestic point was observed (Figure 5). Our findings are consistent with earlier research.[25] The absorption band in the UV region (357 nm, $\varepsilon = 4.14 \times 10^4$ M^{-1} cm^{-1}) was caused by the $\pi \to \pi^*$ transition,[26] while the one emerging upon metal binding in the visible region (438 nm) was attributed to the charge-transfer transition.[27] The observation of a single isosbestic point implies that the binding between **1** and Cu^{2+} produced only a single absorbing complex.[28]

To find the limit of detection (LOD) of **1**, the titration experiment was established (Figure 5a and the detailed calculation in the SI). The LOD was evaluated and calculated to be as low as 0.64 μM Cu^{2+} on the basis of 3SD m^{-1},[29] where SD is the standard deviation of blank measurement and m is the slope of the plot between the absorbance at 438 nm (A_{438}) and Cu^{2+} concentration. This LOD result was much lower than the WHO's (~30 μM or 2 ppm) and US EPA's (~20 μM or 1.3 ppm) maximum allowable amount of Cu^{2+} in drinking water.[11,12,29]

Job's plot analysis was used to further investigate the binding mode of **1** with Cu^{2+}. When the molar fraction was 0.5, the vertical coordinate value was at its highest absorbance (Figure 6), suggesting that the binding stoichiometry between **1** and Cu^{2+} was 1:1. The association constant (K_a) could be determined from the Benesi−Hildebrand plot[30−35] of $1/(A - A_0)$ against $1/[Cu^{2+}]$ (Figure 7) and is found to be 1.49×10^4 M^{-1}.

The LOD and binding constant of a selected hydrazone-based Cu^{2+} probe are compared in Table 1. The LOD range is in μM, and the K_a range is from 10^2 to larger. Our ligand, like other reported compounds, had a low LOD and a high K_a. The majority of ligands in the literature contain substituted benzene rings, with a few compounds containing heterocyclic components like pyridine, pyran, and imidazole. Fluorophores
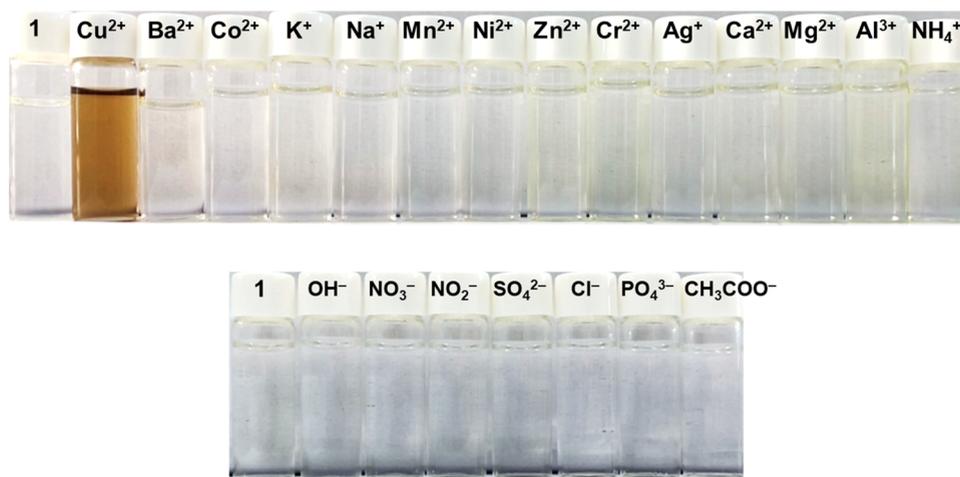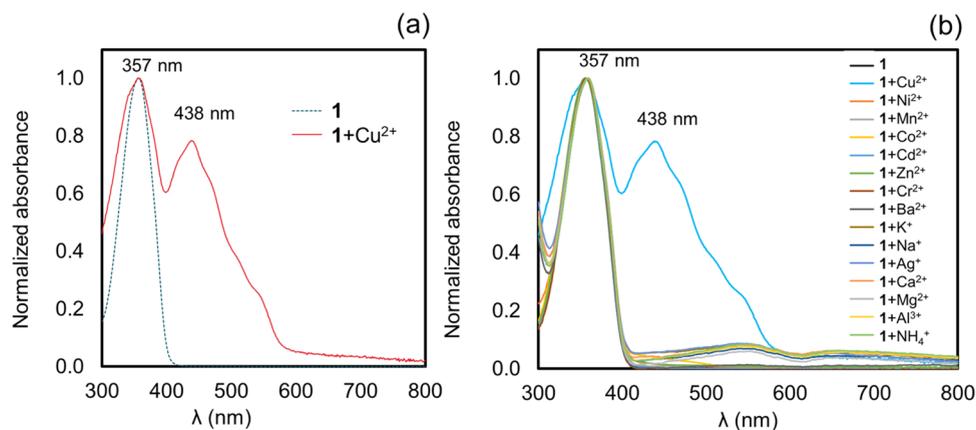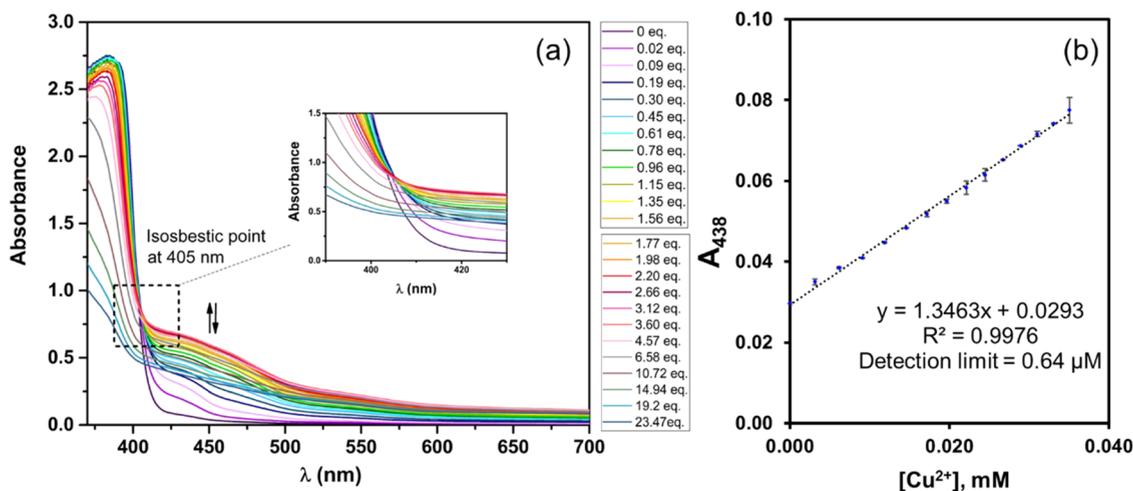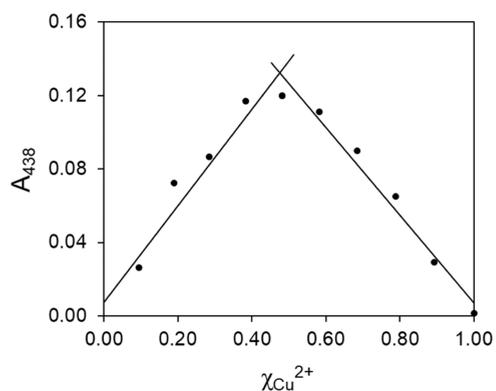

Figure 3. Ethanolic solution (0.54 mM) of **1** and its mixtures with various ions (1:1 v/v). The color changes were observed for only certain metal (Cu^{2+}).

Figure 4. (a) UV−vis spectra of **1** and **1** + Cu^{2+} in ethanol (0.013 mM) and (b) its equimolar mixture of various cations.
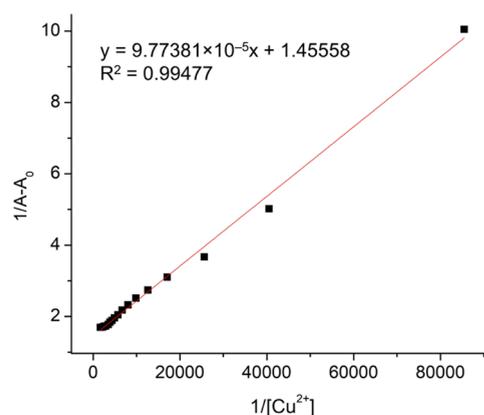

Figure 5. (a) UV−vis spectra of **1** + Cu^{2+} at various mole equivalences (eqs.) showing the isosbestic point at ∼405 nm and (b) titration curve showing the relationship of absorbance (at 438 nm) of the mixture as a function of Cu^{2+} concentration.

Figure 6. Job's plot showing 1:1 complexation of **1** and Cu^{2+}.

Figure 7. Benesi−Hildebrand plot (438 nm) from UV/vis titration data of **1** (0.1603 mM) with Cu^{2+} at various concentrations.

including fluorescein, coumarin, pyrene, and naphthalimide are also added to the structure to improve the fluorescence property of the designed compounds. The complex of **1** and Lewis acid (the cations) is expected to be more rigid and more closely resemble the BODIPY chromophore, resulting in intense photophysical changes. However, the discussion of the binding mode reveals that the **1−Cu** complex did not behave in the same way as BODIPY or BOPHY. Moreover, we have not seen any reports that incorporate the homemade colorimeter with the hydrazone probe in the study. However,

using color data (red−green−blue (RGB) input) derived from the solution color change in a smartphone application is found,[36−44] and it is also a fairly common application for other types of chemosensors.

FTIR analysis of **1** showed the absorption bands corresponding to N−H, C=N, and C−N at 3456, 1644, and 1205 cm^{-1}, respectively (Figure 8). For **1−Cu**, the C=N imine band shifted to the lower wavenumber indicating the

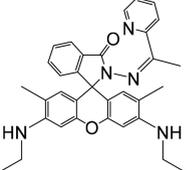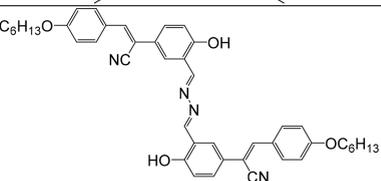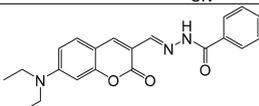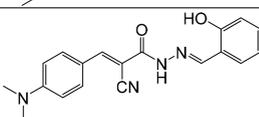**Table 1. Some Reported Properties of Hydrazone-Based Cu^{2+} Chemosensors**

Probe	Detection method	Limit of detection (LOD)	Binding constant (K_a, M^{-1})	Reference
	Fluorometric	0.21 μM	1.8×10^4	31
	Fluorometric	0.108 μM	N/A	32
	Fluorometric	0.1 μM	N/A	33
	Fluorometric	0.439 μM	N/A	34
	Fluorometric	0.039 μM	5.55×10^4	35
	Fluorometric	0.0686 μM	6.579×10^4	36
	Colorimetric	0.20 μM	N/A	37
	Colorimetric	1.871 μM	3.30×10^{10}	38
	Fluorometric	0.9 μM	1.03×10^2	39
	Colorimetric	0.0825 μM	5.72×10^8	40
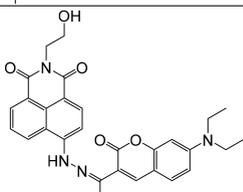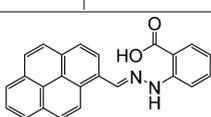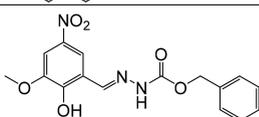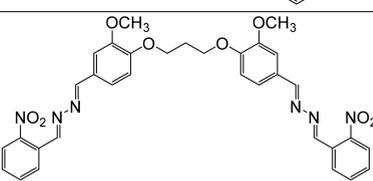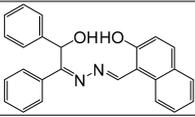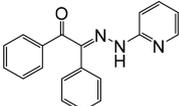
Table 1. continued
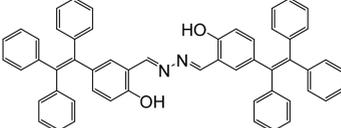
Probe	Detection method	Limit of detection (LOD)	Binding constant (K_a, M^{-1})	Reference
	Fluorometric	0.251 μM	N/A	41
	Colorimetric	28.4 μM	1.87×10^4	42
	Colorimetric	0.080 μM	N/A	43
	Fluorometric	15.14 μM	1.26×10^5	44
	Colorimetric	0.64 μM	1.49×10^4	This work
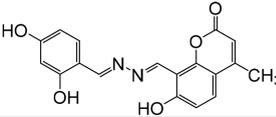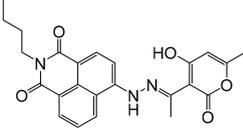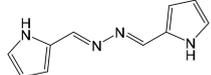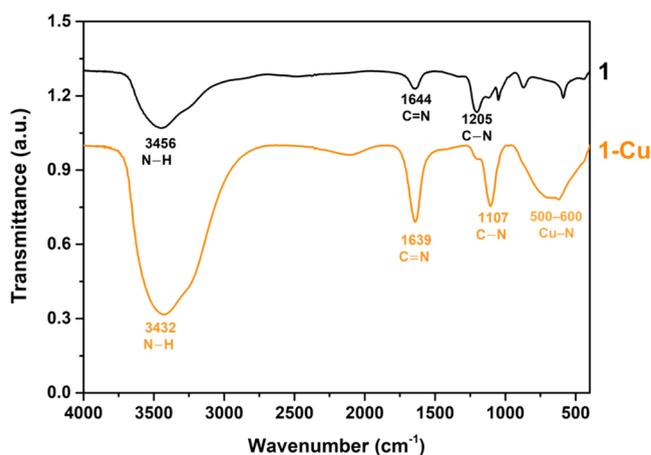
Figure 8. FTIR of **1** (top line) and **1−Cu** (bottom line).

binding mode of Cu−N imine. The C−N band also shifted significantly due to the similar reason of the involvement of *N*-pyrrole and Cu^{2+} complexation. The N−H stretching was also reduced in energy. The total loss of the N−H band, on the other hand, was not seen. This finding might be explained by a partial Cu^{2+} complexation.

Because an excess of Cu^{2+} was added to ensure complete **1−Cu** formation, the presence of the N−H band in the **1−Cu** spectrum could be d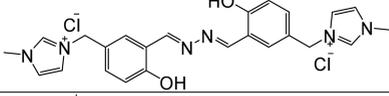ue to complex ion equilibria. And the band at 500−600 cm^{-1} observed in **1−Cu** confirmed the presence of Cu−N in the complex.[45,46]

Compound **1** did not absorb in the visible region, but when Cu^{2+} was added, an absorption band at 438 nm appeared. Furthermore, the addition of the interferences, which are Ba^{2+}, Co^{2+}, K^+, Na^+, Mn^{2+}, Ni^{2+}, Zn^{2+}, Cr^{2+}, Ag^+, Ca^{2+}, Mg^{2+}, Al^{3+}, NH_4^+, OH^-, NO_3^-, NO_2^-, SO_4^{2-}, Cl^-, PO_4^{3-}, and CH_3COO^-, did not cause any significant changes in the absorbance at 438

nm of **1−Cu**. The results in Figure 9 show that the presence of other ions had no effect on compound **1**'s sensory behavior.
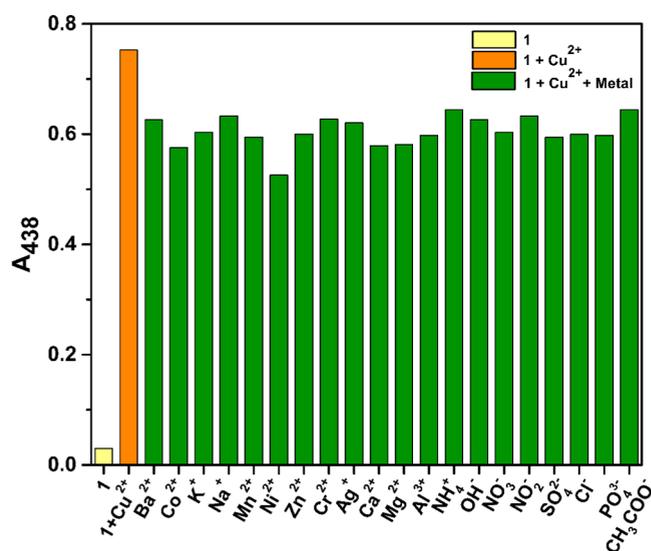
Figure 9. Selectivity and anti-interference effect of **1** for Cu^{2+}.

3.2. Computational Study. The previous work from Yang reported the Cu complex of **1**, which revealed a five-membered chelate ring containing Cu atoms in its crystal structure.[25] However, the BF_2-**1** complex adopted the six-membered-ring chelate formation[14] and the prediction of **1** binding modes with several metal ions are diverse.[47]

Our computational study model adopted the single crystal structure of **1−Cu** from Yang's report. The possible most stable form of the complex was generated from the Crystallographic Information File (CIF). The slightly twisted pyrroles away from the plane were suggested by the optimized molecular geometry of **1−Cu** (Figure 10) with the molecular
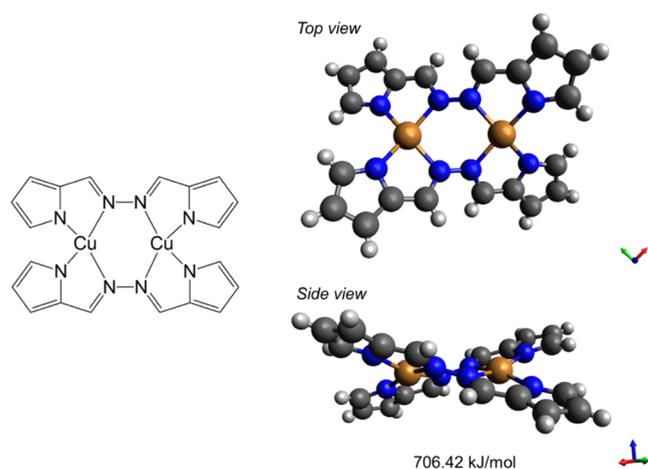
Figure 10. Predicted binding mode and molecular energy of **1−Cu** based on the previously reported crystal structure (Yang's work).[25]

energy of ∼700 kJ/mol. The smaller optimization energy, especially the negative values, implies the better thermodynamic stability of the complex. The optimization energy in the range of a few tens to hundreds of kJ mol^{-1} is observed in some synthesized copper complexes bearing small organic ligands.[48−50]

3.3. Test Strip. To verify the possibility of practical use of **1** as a simple sensor, the paper-based test strips were made and used to detect Cu^{2+}. Compound **1** (50 mg) was dissolved in 20 mL dichloromethane. The solution was then stirred as a piece of filter paper cut into 1×2 cm^2 was added. Subsequently, the soaked paper was air-dried. The dry test strip was evaluated for Cu^{2+} detection ability. When the aqueous Cu^{2+} solution (0.54 mM) came into contact with the paper, the color changed almost quickly from pale yellow to orange (Figure 11a). The same change was observed when the medium ethanolic Cu^{2+} was applied to the testing paper (Figure 11b).
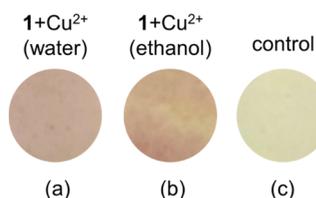

Figure 11. Paper test strip color upon chemosensory testing. The strip before testing appeared yellow (c). (a, b) Paper after applying the aqueous Cu^{2+} and ethanolic Cu^{2+} solution (0.54 mM).

A polymer-based solid matrix was also used to make a composite with compound **1**. Compound **1** (50 mg) was dissolved in 20 mL dichloromethane; then, 300 mg of polylactic acid (PLA) pellet was added into the solution with the aid of stirring. Subsequently, the PLA-**1** composite film was obtained by casting the suspension onto a clean glass slide, evaporating organic solvents, air-drying, and peeling from the glass surface. The Cu^{2+} sensing was performed similar to the case of the paper strip. However, the color change of the polymer composite was not observed (Figure S4).

3.4. Custom-Built Colorimeter. Although high-performance copper quantification techniques are known, the expense of the instruments, such as the atomic absorption spectrophotometer (AAS), is cost prohibitive. Colorimetric chemosensors

provide a more portable and cheap way to analyze the amount of Cu^{2+} in solution. With the feature of LDR, we can acquire the Cu^{2+} concentration with a custom-built colorimeter, which provided a linear relationship between the molar concentration of added Cu^{2+} and the resistance readouts (kΩ, Figure 12).
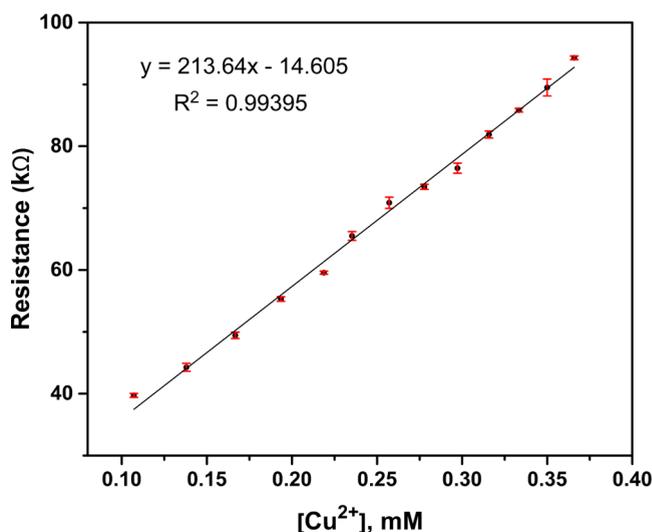
Figure 12. Calibration graph between $[Cu^{2+}]$ presented in the solution and the resistance from the LDR (kΩ).

When additional Cu^{2+} is added, the solution color becomes more intensely orange, resulting in less transmitted light (I, Figure 2). The greater the resistance, the less the light intensity detected at the LDR. For many years, the portable sensing array, sensitivity, and affordability were the determining factors in the development of sensing tools for real-time sample detection.[51,52] Similar to our work, several studies using LED−LDR integrated colorimeters show a good linear relationship between the analyte concentration and electrical signals.[21,53−56] These findings might pave the way for the development of a low-cost test kit that consists of a collection of synthetic ligands for the detection of various contaminants.

3.5. Ligand Stability. One problem for organic chemosensors is the degradation of the compound and poor photostability. The colorimetric signal often diminished over a short period of time due to the unstable complex formation between the analyte and the ligand. We investigate **1−Cu** photostability by monitoring the intensity of the signal peak at 438 nm for ten days (Figure 13). At a low concentration (0.06 mM of **1** and Cu^{2+}), the reduction in A_{438} at around 50% was observed (Table S4). The higher concentration of **1** (0.27 mM) resulted in a greater reduction in A_{438} at >70%, and small brown precipitates, presumed to be the **1−Cu** complex, were observed in the final few days before the experiment was completed. The results indicate that a more diluted solution of **1** would provide better stability for an application.

4. CONCLUSIONS

Compound **1** was successfully synthesized and tested for a chemosensor property. The distinct color changes upon a selective binding with Cu^{2+} ions along with the new absorption band in the visible region were observed. The binding ratio of **1** and Cu^{2+} is 1:1 with the LOD of 0.64 μM (0.040 ppm). The computational study suggested the possible flat complex of **1−Cu** with a mono-six-membered-ring formation with the copper
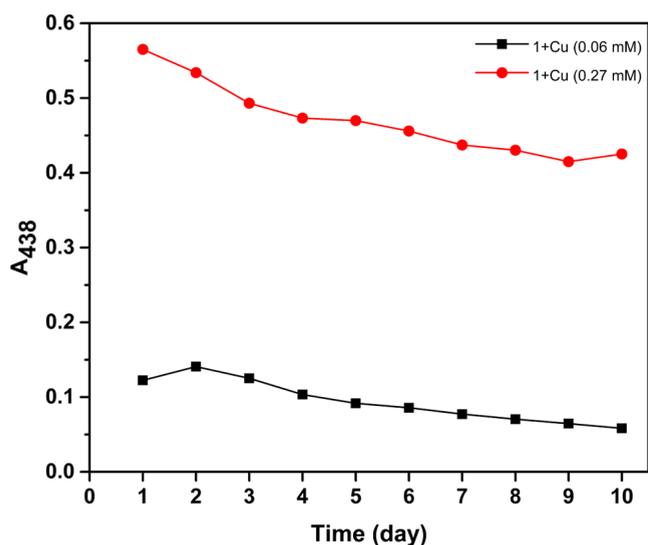
Figure 13. Change in absorbance at 438 nm of **1**−**Cu** with time.

atom. The custom-built colorimeter was assembled and used with the compound to successfully establish the linear relationship between the $[Cu^{2+}]$ and the resistance from the LDR (kΩ). The portable sensing device may be created to monitor the $[Cu^{2+}]$ via the color change of the ligand using this provided concept.

■ ASSOCIATED CONTENT

ⓢ Supporting Information
The Supporting Information is available free of charge at https://pubs.acs.org/doi/10.1021/acsomega.2c06751.

> ^{1}H NMR spectrum of compound 1, spectroscopic data and limit of detection (LOD) calculation, UV−vis spectra of compound 1 + anion mixtures, measured resistance data of a custom-built colorimeter, chemosensor stability test results, picture of PLA-1 films, and spectroscopic data from Benesi−Hildebrand experiment (PDF)

■ AUTHOR INFORMATION

Corresponding Author
Kullapa Chanawanno − *Department of Chemistry, Faculty of Science, Chiang Mai University, Chiang Mai 50200, Thailand; Environmental Science Research Center (ESRC), Chiang Mai University, Chiang Mai 50200, Thailand;* ⓞ orcid.org/0000-0003-2982-4268; Email: kullapa.c@cmu.ac.th

Authors
Sasipan Luangphai − *Department of Chemistry, Faculty of Science, Chiang Mai University, Chiang Mai 50200, Thailand*

Jaturon Fongsiang − *Department of Chemistry, Faculty of Science, Chiang Mai University, Chiang Mai 50200, Thailand*

Pumis Thuptimdang − *Department of Chemistry, Faculty of Science, Chiang Mai University, Chiang Mai 50200, Thailand; Environmental Science Research Center (ESRC), Chiang Mai University, Chiang Mai 50200, Thailand*

Sasiwimon Buddhiranon − *Department of Materials Engineering, Faculty of Engineering, Kasetsart University, Bangkok 10900, Thailand; Department of Polymer Engineering, University of Akron, Akron, Ohio 44325-0301, United States*

Complete contact information is available at:
https://pubs.acs.org/10.1021/acsomega.2c06751

Notes
The authors declare no competing financial interest.

■ REFERENCES
(1) Krüttgen, A.; Cornelissen, C. G.; Dreher, M.; Hornef, M. W.; Imöhl, M.; Kleines, M. Comparison of the SARS-CoV-2 Rapid Antigen Test to the Real Star Sars-CoV-2 RT PCR Kit. *J. Virol. Methods* **2021**, *288*, No. 114024.

(2) Haque, R.; Ali, I. K. M.; Akther, S.; Petri, W. A. Comparison of PCR, Isoenzyme Analysis, and Antigen Detection for Diagnosis of Entamoeba Histolytica Infection. *J. Clin. Microbiol.* **1998**, *36*, 449−452.

(3) Janvier, F.; Sagui, E.; Foissaud, V. ReEBOV Antigen Rapid Test Kit for Ebola. *Lancet* **2015**, *386*, 2254−2255.

(4) Kang, B.; Oh, J.; Lee, C.; Park, B.-K.; Park, Y.; Hong, K.; Lee, K.; Cho, B.; Song, D. Evaluation of a Rapid Immunodiagnostic Test Kit for Rabies Virus. *J. Virol. Methods* **2007**, *145*, 30−36.

(5) Liu, H.; Cui, S.; Shi, F.; Pu, S. A Diarylethene Based Multi-Functional Sensor for Fluorescent Detection of Cd2+ and Colorimetric Detection of Cu2+. *Dyes Pigm.* **2019**, *161*, 34−43.

(6) Tian, J.; Liu, Q.; Asiri, A. M.; Al-Youbi, A. O.; Sun, X. Ultrathin Graphitic Carbon Nitride Nanosheet: A Highly Efficient Fluorosensor for Rapid, Ultrasensitive Detection of Cu 2+. *Anal. Chem.* **2013**, *85*, 5595−5599.

(7) Kang, D. E.; Lim, C. S.; Kim, J. Y.; Kim, E. S.; Chun, H. J.; Cho, B. R. Two-Photon Probe for Cu 2+ with an Internal Reference: Quantitative Estimation of Cu 2+ in Human Tissues by Two-Photon Microscopy. *Anal. Chem.* **2014**, *86*, 5353−5359.

(8) Cui, S.; Pu, S.; Liu, W.; Liu, G. Synthesis and Photochromic Properties of a Multiple Responsive Diarylethene and Its Selective Binding Affinity for Copper(II) Ion. *Dyes Pigm.* **2011**, *91*, 435−441.

(9) Gu, B.; Ye, M.; Nie, L.; Fang, Y.; Wang, Z.; Zhang, X.; Zhang, H.; Zhou, Y.; Zhang, Q. Organic-Dye-Modified Upconversion Nanoparticle as a Multichannel Probe To Detect Cu 2+ in Living Cells. *ACS Appl. Mater. Interfaces* **2018**, *10*, 1028−1032.

(10) Desai, V.; Kaler, S. G. Role of Copper in Human Neurological Disorders. *Am. J. Clin. Nutr.* **2008**, *88*, 855S−858S.

(11) United States Environmental Protection Agency. *National Primary Drinking Water Regulations*, 2009.

(12) World Health Organization. *Guidelines for Drinking-Water Quality*, 2004, Vol. *1*.

(13) Su, X.; Aprahamian, I. Hydrazone-Based Switches, Metallo-Assemblies and Sensors. *Chem. Soc. Rev.* **2014**, *43*, No. 1963.

(14) Tamgho, I.-S.; Hasheminasab, A.; Engle, J. T.; Nemykin, V. N.; Ziegler, C. J. A New Highly Fluorescent and Symmetric Pyrrole−BF 2 Chromophore: BOPHY. *J. Am. Chem. Soc.* **2014**, *136*, 5623−5626.

(15) Li, Y.; Zhou, H.; Yin, S.; Jiang, H.; Niu, N.; Huang, H.; Shahzad, S. A.; Yu, C. A BOPHY Probe for the Fluorescence Turn-on Detection of Cu2+. *Sens. Actuators, B* **2016**, *235*, 33−38.

(16) He, C.; Zhou, H.; Yang, N.; Niu, N.; Hussain, E.; Li, Y.; Yu, C. A Turn-on Fluorescent BOPHY Probe for Cu 2+ Ion Detection. *New J. Chem.* **2018**, *42*, 2520−2525.

(17) Rhoda, H. M.; Chanawanno, K.; King, A. J.; Zatsikha, Y. V.; Ziegler, C. J.; Nemykin, V. N. Unusually Strong Long-Distance Metal-Metal Coupling in Bis(Ferrocene)-Containing BOPHY: An Introduction to Organometallic BOPHYs. *Chem. - Eur. J.* **2015**, *21*, 18043−18046.

(18) Jiang, X.-D.; Su, Y.; Yue, S.; Li, C.; Yu, H.; Zhang, H.; Sun, C.-L.; Xiao, L.-J. Synthesis of Mono-(p-Dimethylamino)Styryl-Containing BOPHY Dye for a Turn-on PH Sensor. *RSC Adv.* **2015**, *5*, 16735−16739.

(19) Sulpizio, C.; Müller, S. T. R.; Zhang, Q.; Brecker, L.; Rompel, A. Synthesis, Characterization, and Antioxidant Activity of Zn2+ and Cu2+ Coordinated Polyhydroxychalcone Complexes. *Monatsh. Chem. - Chem. Mon.* **2016**, *147*, 1871−1881.

(20) Hanwell, M. D.; Curtis, D. E.; Lonie, D. C.; Vandermeersch, T.; Zurek, E.; Hutchison, G. R. Avogadro: An Advanced Semantic Chemical Editor, Visualization, and Analysis Platform. *J. Cheminf.* **2012**, *4*, No. 17.

(21) Santra, D.; Mandal, S.; Santra, A.; Ghorai, U. K. Cost-Effective, Wireless, Portable Device for Estimation of Hexavalent Chromium, Fluoride, and Iron in Drinking Water. *Anal. Chem.* **2018**, *90*, 12815−12823.

(22) O'Donoghue, J. Simplified Low-Cost Colorimetry for Education and Public Engagement. *J. Chem. Educ.* **2019**, *96*, 1136−1142.

(23) Sorouraddin, M. H.; Saadati, M. Determination of Copper in Urine and Water Samples Using a Simple Led-Based Colorimeter. *J. Anal. Chem.* **2010**, *65*, 423−428.

(24) Seetasang, S.; Kaneta, T. Portable Two-Color Photometer Based on Paired Light Emitter Detector Diodes and Its Application to the Determination of Paraquat and Diquat. *Microchem. J.* **2021**, *171*, No. 106777.

(25) Zhang, G.; Yang, L.; Ma, J.; Yang, G. Synthesis and Structural Characterization of 1,2-Bis((1H-Pyrrol-2-Yl)Methylene)Hydrazine and Its Cu(II) Complex. *J. Mol. Struct.* **2011**, *1006*, 542−546.

(26) Ding, H.; Li, B.; Pu, S.; Liu, G.; Jia, D.; Zhou, Y. A Fluorescent Sensor Based on a Diarylethene-Rhodamine Derivative for Sequentially Detecting Cu2+ and Arginine and Its Application in Keypad Lock. *Sens. Actuators, B* **2017**, *247*, 26−35.

(27) Shi, F.; Cui, S.; Liu, H.; Pu, S. A High Selective Fluorescent Sensor for Cu2+ in Solution and Test Paper Strips. *Dyes Pigm.* **2020**, *173*, No. 107914.

(28) Nowicka-Jankowska, T. Some Properties of Isosbestic Points. *J. Inorg. Nucl. Chem.* **1971**, *33*, 2043−2050.

(29) Guo, Z.; Niu, Q.; Li, T.; Sun, T.; Chi, H. A Fast, Highly Selective and Sensitive Colorimetric and Fluorescent Sensor for Cu2+ and Its Application in Real Water and Food Samples. *Spectrochim. Acta, Part A* **2019**, *213*, 97−103.

(30) Aich, K.; Goswami, S.; Das, S. Mukhopadhyay, C. Das. A New ICT and CHEF Based Visible Light Excitable Fluorescent Probe Easily Detects in Vivo Zn 2+. *RSC Adv.* **2015**, *5*, 31189−31194.

(31) Liu, K.; Xu, S.; Guo, P.; Liu, L.; Shi, X.; Zhu, B. A Novel Fluoro-Chromogenic Cu2+ Probe for Living-Cell Imaging Based on Rhodamine 6G-Pyridine Conjugation. *Anal. Bioanal. Chem.* **2019**, *411*, 3021−3028.

(32) Yang, Z.; Yuan, Y.; Xu, X.; Guo, H.; Yang, F. An Effective Long-Wavelength Fluorescent Sensor for Cu2+ Based on Dibenzylidenehydrazine-Bridged Biphenylacrylonitrile. *Anal. Bioanal. Chem.* **2022**, *414*, 4707−4716.

(33) Huang, L.; Cheng, J.; Xie, K.; Xi, P.; Hou, F.; Li, Z.; Xie, G.; Shi, Y.; Liu, H.; Bai, D.; Zeng, Z. Cu2+-Selective Fluorescent Chemosensor Based on Coumarin and Its Application in Bioimaging. *Dalt. Trans.* **2011**, *40*, No. 10815.

(34) Assiri, M. A.; Al-Sehemi, A. G.; Pannipara, M. AIE Based "on-off" Fluorescence Probe for the Detection of Cu2+ Ions in Aqueous Media. *Inorg. Chem. Commun.* **2019**, *99*, 11−15.

(35) Li, C.; Yang, Z.; Li, S. 1,8-Naphthalimide Derived Dual-Functioning Fluorescent Probe for "Turn-off" and Ratiometric Detection of Cu2+ Based on Two Distinct Mechanisms in Different Concentration Ranges. *J. Lumin.* **2018**, *198*, 327−336.

(36) Mukherjee, S.; Betal, S. Sensing Phenomena, Extraction and Recovery of Cu2+ Followed by Smart Phone Application Using a Luminescent Pyrene Based Chemosensor. *J. Lumin.* **2018**, *204*, 145−153.

(37) Park, S.; Choe, D.; Lee, J. J.; Kim, C. A Benzyl Carbazate-Based Colorimetric Chemosensor for Relay Detection of Cu2+ and S2− in near-Perfect Aqueous Media. *J. Mol. Struct.* **2021**, *1240*, No. 130576.

(38) Mohan, B.; Modi, K.; Parikh, J.; Ma, S.; Kumar, S.; Kumar Manar, K.; Sun, F.; You, H.; Ren, P. Efficacy of 2-Nitrobenzylidene-Hydrazine-Based Selective and Rapid Sensor for Cu2+ Ions, Histidine, and Tyrosine: Spectral and Computational Study. *J. Photochem. Photobiol., A* **2022**, *422*, No. 113557.

(39) Bhattacharyya, A.; Ghosh, S.; Makhal, S. C.; Guchhait, N. Hydrazine Appended Self Assembled Benzoin-Naphthalene Conjugate as an Efficient Dual Channel Probe for Cu2+ and F−: A Spectroscopic Investigation with Live Cell Imaging for Cu2+ and Practical Performance for Fluoride. *J. Photochem. Photobiol., A* **2018**, *353*, 488−498.

(40) Hu, S.; Song, J.; Zhao, F.; Meng, X.; Wu, G. Highly Sensitive and Selective Colorimetric Naked-Eye Detection of Cu2+ in Aqueous Medium Using a Hydrazone Chemosensor. *Sens. Actuators, B* **2015**, *215*, 241−248.

(41) Jiang, S.; Qiu, J.; Chen, S.; Guo, H.; Yang, F. Double-Detecting Fluorescent Sensor for ATP Based on Cu2+ and Zn2+ Response of Hydrazono-Bis-Tetraphenylethylene. *Spectrochim. Acta, Part A* **2020**, *227*, No. 117568.

(42) Soufeena, P. P.; Nibila, T. A.; Aravindakshan, K. K. Coumarin Based Yellow Emissive AIEE Active Probe: A Colorimetric Sensor for Cu2+ and Fluorescent Sensor for Picric Acid. *Spectrochim. Acta, Part A* **2019**, *223*, No. 117201.

(43) Zhou, W.; Gao, Q.; Liu, D.; Li, C.; Liu, S.; Xia, K.; Han, B.; Zhou, C. A Single Molecular Sensor for Selective and Differential Colorimetric/Ratiometric Detection of Cu2+ and Pd2+ in 100% Aqueous Solution. *Spectrochim. Acta, Part A* **2020**, *237*, No. 118365.

(44) Saini, N.; Prigyai, N.; Wannasiri, C.; Ervithayasuporn, V.; Kiatkamjornwong, S. Green Synthesis of Fluorescent N,O-Chelating Hydrazone Schiff Base for Multi-Analyte Sensing in Cu2+, F− and CN− Ions. *J. Photochem. Photobiol., A* **2018**, *358*, 215−225.

(45) Dudley, R. J.; Hathaway, B. J.; Hodgson, P. G.; Mulcahy, J. K.; Tomlinson, A. A. G. A Correlation of the Copper-Nitrogen Bond-Lengths, Infrared Spectra and Electronic Spectra of Some Axial Tetraammines and Pentaammines of the Copper(II) Ion. *J. Inorg. Nucl. Chem.* **1974**, *36*, 1947−1950.

(46) Spectroscopic Properties of Inorganic and Organometallic Compounds. In *Spectroscopic Properties of Inorganic and Organometallic Compounds*; Greenwood, N. N., Ed.; Royal Society of Chemistry: Cambridge, 1968; Vol. *1*. DOI: 10.1039/9781847554857.

(47) Dawod, M. M.; Khalili, F. I.; Seyam, A. M. Some Oxovanadium(IV) and Oxozirconium(IV) Complexes of Pyridine-, Pyrrol-, Furan-, and Thiophenaldazine Schiff Bases. *Synth. React. Inorg. Met. Chem.* **1994**, *24*, 663−676.

(48) Anupama, B. DNA Binding Interactions, Docking and Antioxidative Studies of Ternary Copper (II) Complexes. *J. Mol. Struct.* **2020**, *1210*, No. 127988.

(49) Sabolović, J.; Tautermann, C. S.; Loerting, T.; Liedl, K. R. Modeling Anhydrous and Aqua Copper(II) Amino Acid Complexes: A New Molecular Mechanics Force Field Parametrization Based on Quantum Chemical Studies and Experimental Crystal Data. *Inorg. Chem.* **2003**, *42*, 2268−2279.

(50) Rahaman, O.; van Duin, A. C. T.; Bryantsev, V. S.; Mueller, J. E.; Solares, S. D.; Goddard, W. A.; Doren, D. J. Development of a

ReaxFF Reactive Force Field for Aqueous Chloride and Copper Chloride. *J. Phys. Chem. A* **2010**, *114*, 3556−3568.

(51) Sohrabi, H.; Hemmati, A.; Majidi, M. R.; Eyvazi, S.; Jahanban-Esfahlan, A.; Baradaran, B.; Adlpour-Azar, R.; Mokhtarzadeh, A.; de la Guardia, M. Recent Advances on Portable Sensing and Biosensing Assays Applied for Detection of Main Chemical and Biological Pollutant Agents in Water Samples: A Critical Review. *TrAC Trends Anal. Chem.* **2021**, *143*, No. 116344.

(52) Das, R.; Bej, S.; Hirani, H.; Banerjee, P. Trace-Level Humidity Sensing from Commercial Organic Solvents and Food Products by an AIE/ESIPT-Triggered Piezochromic Luminogen and Ppb-Level "OFF−ON−OFF" Sensing of Cu 2+: A Combined Experimental and Theoretical Outcome. *ACS Omega* **2021**, *6*, 14104−14121.

(53) Devamoglu, U.; Duman, I.; Saygili, E.; Yesil-Celiktas, O. Development of an Integrated Optical Sensor for Determination of β-Hydroxybutyrate Within the Microplatform. *Appl. Biochem. Biotechnol.* **2021**, *193*, 2759−2768.

(54) Hoang, L. Q.; Chi, H. B. L.; Khanh, D. N. N.; Vy, N. T. T.; Hanh, P. X.; Vu, T. N.; Lam, H. T.; Phuong, N. T. K. Development of a Low-Cost Colorimeter and Its Application for Determination of Environmental Pollutants. *Spectrochim. Acta, Part A* **2021**, *249*, No. 119212.

(55) Fatoni, A.; Aziz, A. N.; Anggraeni, M. D. Low-Cost and Real-Time Color Detector Developments for Glucose Biosensor. *Sens. Bio-Sensing Res.* **2020**, *28*, No. 100325.

(56) Mandal, N.; Mitra, S.; Bandyopadhyay, D. Paper-Sensors for Point-of-Care Monitoring of Drinking Water Quality. *IEEE Sens. J.* **2019**, *19*, 7936−7941.